Pergamon

Int. J. Heat Mass Transfer. Vol. 40, No. 17, pp. 4105–4114, 1997

Printed in Great Britain
0017–9310/97 $17.00+0.00

PII: S0017–9310(97)00068–9

Convection in a long cavity with differentially heated end walls

BERTRAM BOEHRER†

Institut für Mechanik AG 3, Technische Hochschule, Hochschul-Str. 1, D-64289 Darmstadt, Germany

(*Received* 28 *June* 1996 *and in final form* 3 *February* 1997)

Abstract—The fluid-filled long cavity with differentially heated end walls is a common and simple model for flows both in the environment and in technical applications. A delineation of the flow regime showing confined flowing layers from those showing cavity-filling counter currents is provided. Theoretical considerations yield a description of the flowing layer thickness and an approximate value for the longitudinal temperature gradient in the core of the tank. This way, a good description of the major features in the long cavity is achieved, which is confirmed by experimental data. © 1997 Elsevier Science Ltd.

1. INTRODUCTION

Buoyancy driven flows in cavities with a low aspect ratio are common in the environment and in industrial applications. The classic example in the environment is the estuary which is connected to water masses of different densities at either end. Flows through channels and straits can be buoyantly controlled. Similar flows occur in technical applications, such as convection flows in low horizontal gaps, solar collectors and water or fuel tanks. Furthermore, the air circulation in rooms and the ventilation of ducts, as well as the coolant flow in heat exchangers, could be named. In these examples, the Rayleigh number Ra, the Prandtl number Pr and the aspect ratio A (defined below) cover a wide range of values and as some of the values are difficult to reproduce in laboratory studies, extrapolations from experiments have to be made to draw conclusions.

The first investigations on convection flows in a side cavity (see also sketch in Fig. 1) concentrated on the case where the height exceeded the length [1, 2]. Various flow regimes were found, for example the regime boundary for a core between the two boundary layers next to the heated and cooled walls. Their approach was the starting point for later investigations on different geometries.

The problem of the long cavity with differently heated end walls has received considerable attention over the last 25 years, but it is still too early to claim that the various flow regimes are understood or that the regime boundaries are known. Hart [3] was the first to find the simple solution of a cubic profile for the baroclinically driven flow through a long rectangular tube with a longitudinal buoyancy gradient. Cormack *et al.* [4, 5] and Imberger [6] used a perturbation solution and matched the core solution with a solution valid in the end regions. They concluded $K_1 = (\delta T/l)/(\Delta T/L)$ should deviate from 1 if $Ra^2A^3 > 10^5$.

Soon afterwards Bejan and Tien [7] proposed a division into three flow regimes (see Fig. 2), which they called the $Ra \to 0$ regime (here: conductive regime), the intermediate regime (here: transition regime) and the boundary–layer regime (here: convective regime). They approached the problem mainly by investigating the heat transfer and concluded from theoretical considerations and experimental results that the regime boundaries could be found at $Ra \approx 72A^{-2}$ and $Ra \approx 4.4 \times 10^4 A^{-5/3}$, respectively. Later publications (e.g. Bejan [8]), never referred to three flow regimes and work continued on just the regime boundary concerning the transition of the velocity profile, whether a space of thickness J (non-dimensionalised by cavity height H, Fig. 2, right-hand upper panel) could form between the intrusions or disappeared. The case of a low Prandtl number fluid was investigated in Hart [9] and Drummond and Korpela [10]; in the latter also, the cases of different boundary conditions (perfectly conducting horizontal boundaries) along the horizontal surfaces was considered.

Patterson and Imberger [11] searched a mathematical description of the layer thickness in the core for the case of high Rayleigh number, where distinct flowing layers were found. They scaled the thickness by assuming that the discharge through a cross-section equals the discharge of a hot vertical plate in a homogeneous environment. The velocity was based on a buoyancy–viscosity balance and under these assumptions they found a layer thickness of $\delta/H \sim$

† Present address: UFZ-Gewässerforschung, Am Biederitzer Busch 12, D-39114 Magdeburg, Germany.

NOMENCLATURE

a	$=360/RaA^2$
A	$=H/L$, aspect ratio
g	acceleration due to gravity
H	height of cavity
J	non-dimensional thickness of stagnant fluid
K_1	$=(\delta T/l)/(\Delta T/L)$, bulk value of the non-dimensional horizontal temperature gradient over the middle section of the cavity
l	distance in x-direction
L	length of cavity
$\mathscr{L}$	$=-a-\sqrt{a^2+2a}$, lower bound for K_1
p	pressure
Pr	$=\nu/\kappa$, Prandtl number
Q	dishcarge [$m^2\ s^{-1}$]
Ra	$=g\alpha\Delta TH^3/(\nu\kappa)$, Rayleigh number
t	time
T	temperature
u	horizontal velocity, parallel x
U	horizontal velocity scale
$\mathscr{U}$	$=-a+\sqrt{a^2+2a}$, upper bound for K_1
x	horizontal coordinate
z	vertical coordinate, antiparallel to gravity.

Greek symbols

α	thermal expansion coefficient
δ	flowing layer thickness
δT	temperature difference between two points inside the cavity
ΔT	temperature difference between hot and cold wall
ΔT_{t-b}	temperature difference between top and bottom in the core of the tank
	thermal diffusivity
κ	thermal diffusivity
ν	kinematic viscosity
ρ	density
τ_a	$=L/U$, time scale for horizontal advection
τ_c	$=H^2/\kappa$, time scale for vertical thermal conduction.

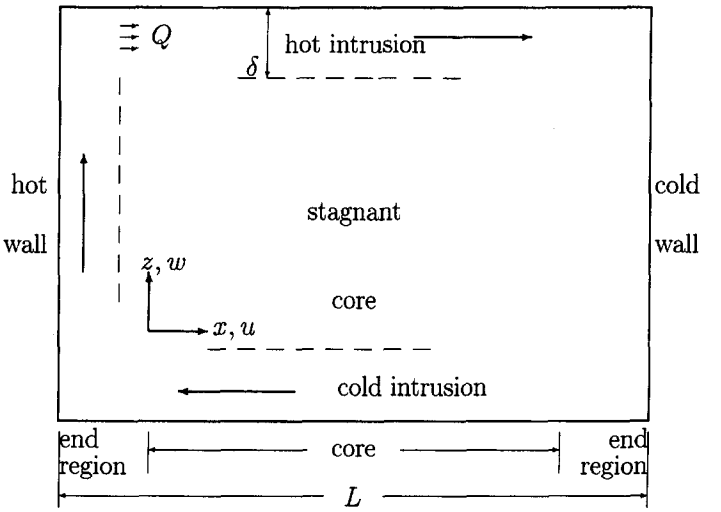

Fig. 1. Sketch of a side-heated cavity.

$Ra^{-3/16}A^{-1/4}$ which is valid as long as $Ra > A^{-12}$; the transition from the convective regime to the transition regime would be, when $\delta/H \sim 1$. The agreement with experimental data was very good and it is the most generally accepted scaling in the square cavity (e.g. Henkes and Hoogendoorn [12], Henkes [13]).

Bejan *et al.* [14] performed experiments with water as the working fluid and they found distinct boundary layers close to the bounding horizontal surfaces of the long cavity. Measuring velocity profiles, they were able to draw streamlines which indicated that entrainment happened as the intrusion was traversing the cavity. Using scaling arguments, they compared the heat discharge from the hot plate with vertical temperature diffusion and concluded that confined flowing layers should occur for $Ra^{1/4}A > 1$. Experiments from various authors were cited which supported their regime boundary quite strongly.

Simpkins and Dudderar [15] approached the regime boundary experimentally and contributed several important experiments in a long cavity for high Pr as did Simpkins and Chen [16] for $Pr = 7$. Including these new results, Ivey and Hamblin [17] realized that the regime boundary $Ra^{1/4}A \approx 1$ could be supported no longer. Hence, the comparison of heat fluxes was not the correct approach for deriving the regime

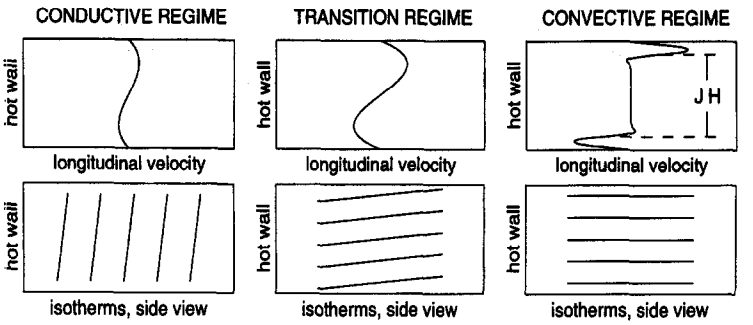

Fig. 2. Sketches of longitudinal velocity (upper row) and several isotherms (lower row) in a side view of a long tank for the three flow regimes. J represents the thickness of the stagnant cores as a portion of the cavity height H.

boundary for the flow field and it was replaced by the comparison of the advective momentum transport with the momentum loss by viscous friction which occurred while the intrusion was traversing the tank. These arguments yielded the regime boundary $Ra^{1/4}A \sim Pr$.

In conclusion, for the long cavity ($Ra < A^{-12}$) the flow features in the conductive regime are known, with the solution by Hart [3] and Cormack *et al.* [4], where $K_1 \approx 1$. In the transition regime, K_1 varies and a description for K_1 which is based only on Ra, A and Pr would be desirable. Finally, in the convective regime a mathematical description of the flowing layer thickness is still being looked for. This publication tries to find answers to both questions and theoretically-based arguments will be critically compared with the available experimental results.

2. AVAILABLE DATA

The long cavity with differentially heated end walls is fully characterized by three numbers: the Rayleigh number, the Prandtl number and the aspect ratio:

$$Ra = \frac{g\alpha\Delta T H^3}{\kappa\nu} \quad Pr = \frac{\nu}{\kappa} \quad A = \frac{H}{L} \tag{1}$$

where α, ν and κ are the fluid properties of thermal expansion, viscosity and thermal conductivity, respectively, H and L the height and the length of the cavity and ΔT the applied temperature difference between the heated and cooled plate and finally g is the acceleration due to gravity.

We searched the literature for experimental and numerical runs which were conducted at low enough aspect ratio that the following inequalities were fulfilled: $0 < A \leqslant 0.25$ for the low aspect ratio, $Ra < A^{-12}$ to investigate the flows beyond the validity of Patterson and Imberger's [11] study and $Pr > 1$, so that a viscous velocity scale can be assumed for an intrusion of a conductively controlled thickness (see below). The runs were included in Table 1, where we used the experiment names chosen by the original authors. The values for K_1 were given in most publications, if not they can easily be calculated from the published information. The value for J was inferred from the published velocity profiles at a central location. J is the portion of the entire height measured from the upper point of inflection to the lower point of inflection in the velocity profile. Two experiments were mentioned with 'strong jets' (Bejan *et al.* [14]), but the velocity profile could not be recovered and, hence, they were included with $J = 0.75 \pm 0.25$ and an error bar, when used in the plots.

Also included are the data from Böhrer [18], which are the first measurements of K_1 within the desired parameter range at a Prandtl number different from $Pr = 7$. The experiments were run in a rectangular tank of length 1.08 m and width 0.36 m. He used glycerol as the working fluid and measured its viscosity to determine the water content (~ 1 or 3%, respectively) of the mixture. Then the values for thermal conductivity and thermal expansion could be read from tables quite accurately. K_1 was calculated as the difference of temperatures at $x/L = 0.25$ and $x/L = 0.75$ at mid-height and a lateral position close to central.

3. VELOCITY STRUCTURE

We start our theoretical considerations with a motivation of the parameter RaA^2, which, as we will show, will play a central role in the long cavity. For the long cavity, there are two important time scales, τ_c the time scale for the vertical conduction and the advective time scale τ_a

$$\tau_c = \frac{H^2}{\kappa} \quad \tau_a = \frac{L}{U}. \tag{2}$$

U, a velocity scale for the advection in the tank, can be derived from a buoyancy–viscosity balance in the usual way:

$$0 = -\frac{1}{\rho}\cdot\frac{\partial p}{\partial x} - \tau\frac{\partial^2 u}{\partial z^2} \tag{3}$$

$$0 = -\frac{1}{\rho}\cdot\frac{\partial p}{\partial z} - g\alpha T. \tag{4}$$

Table 1. The published data from experimental and numerical runs including the non-dimensional parameters Ra, A and Pr, the criterion RaA^2 and the non-dimensionalized values of the measured magnitudes of K_1 and J (definition below). $J(I3) = 0.2$ from Imberger [23]

Author	exp	$Ra \times 10^{-6}$	A	Pr	RaA^2	$K_1 = \frac{\delta T/l}{\Delta T/L}$	J
Imberger [6]	I4	8.04	0.019	7	2900	0.21	0
	I2	14.1	0.019	7	5000	0.16	0
	I1	33.5	0.019	7	12 000	0.08	0
	I3	111	0.019	7	40 000	0.05	0.2
	I5	1.31	0.01	7	130	0.75	0
	I6	2.34	0.01	7	230	0.58	0
	I7	4.75	0.01	7	330	0.40	0
	I8	12.2	0.01	7	1200	0.28	0
Cormack *et al.* [5] (numerical)	C3	0.14	0.2	7	5600	0.116	0
	C4	0.14	0.1	7	1400	0.336	0
	C5	0.14	0.05	7	360	0.603	0
	C6	0.014	0.1	7	140	0.840	0
	C7	0.0035	0.1	7	35	0.968	0
	C8	0.00007	0.1	7	0.64	0.996	0
Kumar and Ostrach [19]	K1	0.03	0.1	963	290	—	0
	K2	0.065	0.1	963	630	—	0
	K3	0.11	0.1	963	1090	—	0
Al-Homoud and Bejan [20]	A1	290	0.0625	7	1.14×10^6	0	—
	A2	841	0.0625	7	3.3×10^6	−0.02	—
	A3	1220	0.0625	7	4.8×10^6	−0.02	—
Bejan *et al.* [14]	B1	200	0.0625	7	0.78×10^6	—	0.75 ± 0.25
	B2	1590	0.0625	7	6.2×10^6	—	0.75
Loka [21]	L1	13.5	0.2	1380	0.54×10^6	—	0.5
Ostrach *et al.* [22]	L2	18	0.2	1380	0.72×10^6	—	0.75 ± 0.25
	L3	1.92	0.1	1380	19 000	—	0
	L4	0.29	0.05	1380	730	—	0
Simpkins and Dudderar [15]	S1	5.4	0.25	105	0.34×10^6	—	0.5
	S2	3.0	0.25	105	0.19×10^6	—	0.3
Simpkins and Chen [16]	S3	1.3	0.25	7	0.81×10^6	—	0.3
	S4	9	0.25	7	0.56×10^6	—	0.6
Böhrer [18]	G0	0.11	0.035	84	130	0.6	—
	H0	1.06	0.087	54	8100	0.14	—

z is the coordinate antiparallel to the gravity force, x and u are referred to as horizontal coordinate and horizontal velocity, respectively. ρ is the fluid density and p the pressure. Cross-differentiate, the pressure term cancels out and, as we aim for a characterization of the cavity rather than of the intrusions, we use the scales H for z, L for x, ΔT for T and U for u and we finish with the scale

$$U \sim \frac{g\alpha \Delta T H^3}{\nu L} \sim Ra \frac{\kappa}{L} \tag{5}$$

which means

$$RaA^2 \sim \frac{\tau_c}{\tau_a} \tag{6}$$

is a measure for the relative importance of horizontal advection compared to vertical conduction of heat in a fluid body where viscous horizontal velocities prevail.

3.1. *Theoretical considerations*

For the thickness δ of the intruding thin flowing layers in the boundary-layer regime, usually the criterion by Patterson and Imberger [11] is applied (e.g. Henkes and Hoogendoorn [12]), where the discharge of the hot vertical plate $Q \sim \kappa Ra^{1/4}$ is considered to match the discharge through any cross-section in the tank throughout the length of the cavity. For the velocity scale, they use a buoyancy viscosity balance and regard δ (instead of H in equation (5)) as the crucial length scale which yields a velocity:

$$U \sim \frac{g\alpha \Delta T \delta^3}{\nu L} \sim Ra \frac{\kappa}{L} \left(\frac{\delta}{H}\right)^3 \tag{7}$$

and, thus, derive a layer thickness:

$$\frac{\delta}{H} \sim \frac{Q}{UH} \sim Ra^{-3/16} A^{-1/4}. \tag{8}$$

Experimental and numerical results support this scale very well in the square cavity, and Patterson and Imberger [11] claim it to be valid, as long as $Ra > A^{-12}$.

In a long cavity, the result could be quite different. After propagating through a long tank, the intrusion layer might be altered due to viscous and conductive processes to an extent that the discharge through a cross-section might deviate from the discharge of the hot plate. Bejan *et al.* [14] measured velocity profiles in a long cavity at various locations and based on the

velocity information they were able to draw streamlines in the tank, indicating that entrainment happens.

Similar to the (modified) Bejan *et al.* approach (see Appendix), we also assume that the thickness of the flowing layers close to the horizontal boundaries are conductively controlled, i.e. $\delta \sim \sqrt{\kappa t}$. We use the advective time scale $\tau_a = L/U$ [see equation (2)] and use the viscous velocity scale based on the layer thickness [equation (7)], as the flow is controlled by viscosity, as long as $\sqrt{\nu t} > \delta = \sqrt{\kappa t} \Rightarrow Pr > 1$. This yields the flowing layer thickness δ in non-dimensional form:

$$\frac{\delta}{H} \sim (RaA^2)^{-1/5}. \tag{9}$$

In a cavity the conductive thickness [equation (9)] will be important, if it exceeds the thickness implied by the discharge from the hot wall [equation (8)] which is equal to:

$$Ra < A^{-12} \tag{10}$$

and confirms Patterson and Imberger's boundary for the validity of their scaling. The transition from confined flowing layers to cavity filling counter currents happens when $\delta \sim H/2$.

3.2. *Verification*

To verify our scale for the thickness of the flowing layer, we plot the non-dimensional flowing layer thickness $(1-J)/2$, measured from the experiments, vs RaA^2 (Fig. 3) and include the scaled estimate $\delta/H = 3.2 \cdot (RaA^2)^{-1/5}$. The experimental data show $\delta/H = 0.5$ at low values of RaA^2, then its value falls rapidly and consistently from a point $RaA^2 \approx 1 \times 10^4$. The scaled estimate shows a similar behaviour for $RaA^2 > 10^4$ and the differences between measured and scaled estimates are within the accuracy of the measurements. For $RaA^2 < 10^4$ the scaling would predict a flowing layer thickness of $\delta/H > 0.5$, which is physically not possible and cavity filling counter currents are found. Plots of the experimental data vs other possible criteria are provided in Appendix A, proving that the conductive layer thickness is the much better description than the also possible viscous layer thickness.

4. TEMPERATURE STRUCTURE

A parameter of central importance in the transition regime ($10^2 < RaA^2 < 10^4$) is the longitudinal temperature gradient along the main axis of the tank. Knowing its value would supply the information necessary for the determination of flow speed as well as vertical temperature structure in the solution by Cormack *et al.* [4]. By simple means it will be shown that an upper limit can be found, which has strong implication for the actual value. By dividing the RaA^2 domain up into three regimes, approximate values can be provided.

4.1. *Theoretical considerations and experimental verification*

As the first step, we refer to the results from Cormack *et al.* [4, 5] and Imberger [6]. They introduced the non-dimensional temperature gradient $K_1 = (\delta T/l)/(\Delta T/L)$ which stood for the portion of the end wall temperature difference that contributed to a longitudinal temperature gradient in the core of a tank. They performed a perturbation solution of the Navier–Stokes–Fourier equations where viscosity and vertical diffusion governed the problem, which is valid, as they showed, for values of RaA^2 as large as 10^4. Here we borrow their result for the temperature difference between top and bottom at the same horizontal location x:

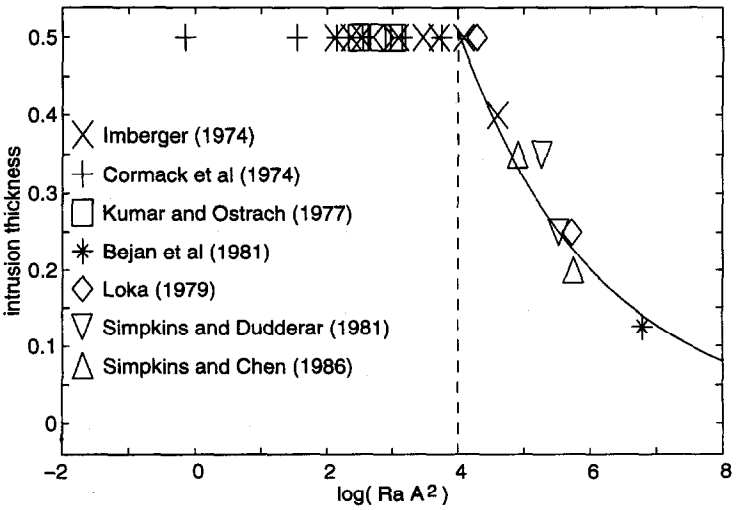

Fig. 3. Intrusion thickness δ/H vs RaA^2. The experimental values decrease monotonically from a point $RaA^2 \approx 1 \times 10^4$ (broken line). The solid line is based on the above scaling and shows the function $\delta/H = 3.2 \cdot (RaA^2)^{-1/5}$.

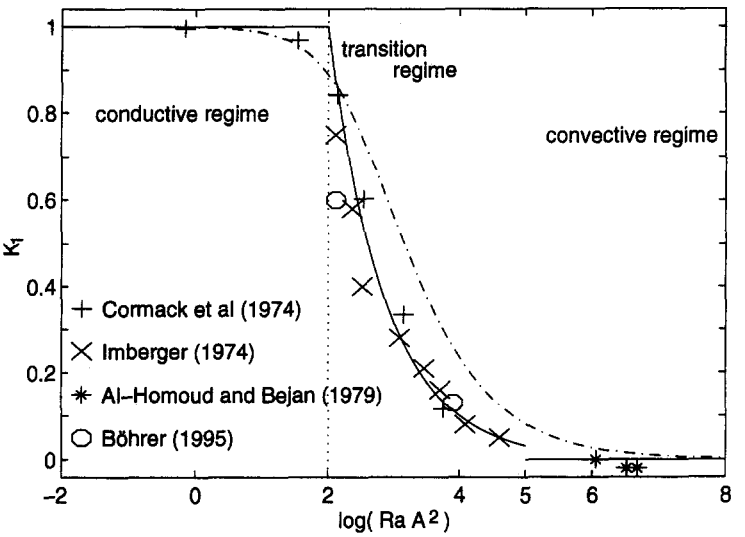

Fig. 4. The upper limit ($\mathscr{U}$ dash–dotted line) for the longitudinal temperature gradient K_1 and the experimental results (symbols). The dotted line delineates the conductive regime from the transition regime and the convective regime, while the solid lines represent the approximate values for K_1.

$$\Delta T_{t-b} = \tfrac{1}{720} K_1^2 RaA^2 \Delta T. \tag{11}$$

It is clear that in the long box the temperatures inside the cavity are between the temperatures implied by the walls and, hence, we assume:

$$\Delta T_{t-b} + K_1 \Delta T \leqslant \Delta T. \tag{12}$$

This equation is second-order in K_1 and possesses real solutions K_1, if:

$$\mathscr{L} := -a - \sqrt{a^2+2a} \leqslant K_1 \leqslant -a + \sqrt{a^2+2a} := \mathscr{U} \tag{13}$$

where we used $360/RaA^2 = a$ for convenience. While it is not clear, whether the lower boundary ($\mathscr{L}$) has any physical implication, the upper boundary ($\mathscr{U}$) limits the values for K_1 and, hence, the experimental data should reflect this conjecture (see Fig. 4).

Looking at equation (13), we find we can make a Taylor expansion of the square root for two cases $a \ll 2$ and $a \gg 2$, which is tantamount to considering either one of the two left-hand side terms in equation (12) as the leading term. For the conductive regime $RaA^2 \ll 100$, we assume $K_1 \Delta T \sim \Delta T$ and, hence:

$$K_1 \approx 1 \tag{14}$$

and from $\Delta T_{t-b} \leqslant \Delta T$, we conclude $K_1 \leqslant (RaA^2/720)^{-1/2}$ for the transition regime. We find the actual values are a factor 2.7 lower, a factor which in good approximation is constant over the entire domain where experimental data are available:

$$K_1 \approx 10(RaA^2)^{-1/2}. \tag{15}$$

This approximation has a theoretical justification only in the transition regime ($RaA^2 < 10^4$). Beyond that, confined flowing layers start to establish and far in the convective regime ($RaA^2 > 10^5$), the fluid at mid-height is not driven buoyantly and, therefore, it can be expected to have a vanishing longitudinal temperature gradient

$$K_1 \approx 0. \tag{16}$$

The approximations for K_1 [equations (14)–(16)] are represented in Fig. 4 by solid lines.

Previously it had been stated that the longitudinal temperature gradient in the long cavity is determined by boundary conditions implied by the end regions (Cormack *et al.* [4–6]) or can be derived as a consequence of instabilities happening close to the end walls [24]. Both criteria are used in the displays of Appendix B for comparison.

5. CONCLUSION

We investigated the flow in a long cavity with differentially heated end walls, with the aspect ratio A low enough that the following inequalities are fulfilled: $0 < A < 0.25$ and $Ra < A^{-12}$, as well as $Pr > 1$. We found the governing parameter for the longitudinal temperature gradient and for the thickness of the flowing layers was RaA^2. This implied that the governing processes in the long cavity were vertical conduction of heat and longitudinal viscous advection. Based on this criterion, we proposed a division into three flow regimes (Fig. 2): the conductive regime, the transition regime and the convective regime. The regime boundaries could be found at $RaA^2 = 10^2$ and $RaA^2 = 10^4$, respectively.

In the convective regime, we confirmed thin flowing layers along the lid and the bottom of the cavity with a thickness of $\delta/H \approx 3.2(RaA^2)^{-1/5}$. This scale was based on a conductive thickness and all experiments agreed with it (Fig. 3). For values $RaA^2 < 10^4$ (tran-

sition regime and conductive regime), a layer thickness of more than half the cavity height ($H/2$) would be predicted and we found cavity-filling counter currents. Low values for RaA^2 indicated enhanced exchange of heat in the vertical between the hot and the cold currents and a longitudinal temperature gradient was the logical consequence.

We could provide an upper limit for the value of the longitudinal temperature gradient K_1 on the main axis of the tank, based on the Hart [3] and Cormack *et al.* [4] solution. A confirmation with the available data was provided (Fig. 4). The temperature gradient on the tank's main axis $K_1 \approx 1$ in the conductive regime, $K_1 \approx 10(RaA^2)^{-1/2}$ in the transition regime which was a good approximation into the convective regime up to $RaA^2 = 10^5$, above which the longitudinal temperature gradient was very weak ($K_1 \approx 0$).

With the above results for K_1, the Hart [3] and Cormack *et al.* [4] core solution is applicable in the conductive regime and the transition regime, where the velocity field and the temperature field are functions of outside parameters only. Replacing formally Ra by the Darcy–Rayleigh number, we find a strong analogy with the convection through porous media contained in a long cavity (see Blythe *et al.* [25]). The present contribution together with Gill [2] and Patterson and Imberger [11] allow one to judge whether a stagnant core can form in a side-heated cavity of any aspect ratio (see Boehrer [26]).

Acknowledgements—The helpful comments on the drafts by Dr Michael Coates, Dr Bernhard Hürzeler and Professor K. Hutter are gratefully acknowledged. I would also like to thank Professor P. G. Simpkins, Professor A. Bejan, Professor J. Imberger, Professor J. Patterson and Professor G. N. Ivey for the discussions about the previous work. The work was partly funded by an Overseas Postgraduate Research Scholarship (OPRS) and a University Research Scholarship (URS) of the University of Western Australia.

REFERENCES

1. Batchelor, G. K., Heat transfer by free convection across a closed cavity between vertical boundaries at different temperatures. *Quarterly Applied Mathematics*, 1954, **12,** 209–233.
2. Gill, A. E., The boundary layer regime for convection in a rectangular cavity. *Journal of Fluid Mechanics*, 1966, **26,** 515–536.
3. Hart, J. E., Stability of thin non-rotating Hadley circulations. *Journal of Atmospheric Science*, 1972, **9,** 687–697.
4. Cormack, D. E., Leal, L. G. and Imberger, J., Natural convection in a shallow cavity with differentially heated end walls, Part 1, analytical solution. *Journal of Fluid Mechanics*, 1974, **65,** 209–229.
5. Cormack, D. E., Leal, L. G. and Seinfeld, J. H., Natural convection in a shallow cavity with differentially heated end walls, Part 2, numerical results. *Journal of Fluid Mechanics*, 1974, **65,** 230–246.
6. Imberger, J., Natural convection in a shallow cavity with differentially heated end walls, Part 3, experimental results. *Journal of Fluid Mechanics*, 1974, **65,** 247–260.
7. Bejan, A. and Tien, C. L., Laminar natural convection heat transfer in a horizontal cavity with different end temperatures. *ASME, Journal of Heat Transfer*, 1978, **100,** 641–647.
8. Bejan, A., *Convective Heat Transfer*, 2nd edn. Wiley, New York, 1995.
9. Hart, J. E., Low Prandtl number convection between differentially heated end walls. *International Journal of Heat and Mass Transfer*, 1983, **26,** 1069–1074.
10. Drummond, J. E. and Korpela, S. A., Natural convection in a shallow cavity. *Journal of Fluid Mechanics*, 1987, **182,** 543–564.
11. Patterson, J. C. and Imberger, J., Unsteady natural convection in a rectangular cavity. *Journal of Fluid Mechanics*, 1980, **100**(1), 65–86.
12. Henkes, R. A. W. M. and Hoogendoorn, C. J., Scaling of the laminar natural-convection flow in a heated square cavity. *International Journal of Heat and Mass Transfer*, 1993, **36**(11), 2913–2925.
13. Henkes, R. A. W. M., Natural convection boundary layers. Ph.D. thesis, Technische Universiteit Delft, Netherlands, 1990.
14. Bejan, A., Al-Homoud, A. and Imberger, J., Experimental study of high Rayleigh number convection in a horizontal cavity with different end temperatures, *Journal of Fluid Mechanics*, 1981, **109,** 283–299.
15. Simpkins, P. G. and Dudderar, T. D., Convection in rectangular cavities with differentially heated end walls. *Journal of Fluid Mechanics*, 1981, **110,** 433–456.
16. Simpkins, P. G. and Chen, K. S., Convection in horizontal cavities. *Journal of Fluid Mechanics*, 1986, **166,** 21–39.
17. Ivey, G. N. and Hamblin, P. F., Convection near the temperature of maximum density for high Rayleigh number, low aspect ratio, rectangular cavities. *Journal of Heat Transfer*, 1989, **111,** 100–104.
18. Böhrer, B., Convection in a rotating, long. Ph.D. thesis, University of Western Australia, Nedlands, WA 6907, Australia, 1995.
19. Kumar, A. and Ostrach, S., Case Western Reserve University, Department of Mechanical Aerospace Engineering Report, FTAS/TR-77-132 (from citation [14]), 1977.
20. Al-Homoud, A. A. and Bejan, A., Experimental study of high Rayleigh number convection in horizontal cavity with different end temperatures, CUMER-79-1 (from Bejan, personal communication and citation [14]), 1979.
21. Loka, R. R., M.S. thesis, Department of Mechanical and Aerospace Engineering, Case Western Reserve University (from citation [22]), 1979.
22. Ostrach, S., Loka, R. R. and Kumar, A., Natural convection in low aspect ratio rectangular enclosures. *19th National Heat Transfer Conference*, Orlando, Florida, 1980.
23. Imberger, J., personal communication, Notes on [6], BOX 7/1, R6, Centre for Water Research, Nedlands 6907, Australia.
24. Daniels, P. G., High Rayleigh number thermal convection in a shallow laterally heated cavity. *Proceedings of the Royal Society London A*, 1993, **440,** 273–289.
25. Blythe, P. A., Simpkins, P. G. and Daniels, P. G., Thermal convection in a cavity filled with a porous medium: a classification of limiting behaviours. *International Journal of Heat and Mass Transfer*, 1983, **26**(5), 701–708.
26. Boehrer, B., Necessary conditions for a stagnant core in the side heated cavity. *Fifth Australian Natural Convection Workshop*, December 1996, Department of Mechanical and Mechatronic Engineering, University of Sydney, Sydney 2006, 1996.

APPENDIX A

Flowing-layer thickness vs other possible criteria

In this paper, we claim that the best parameter to describe the occurrence of the stagnant fluid body is RaA^2. In order

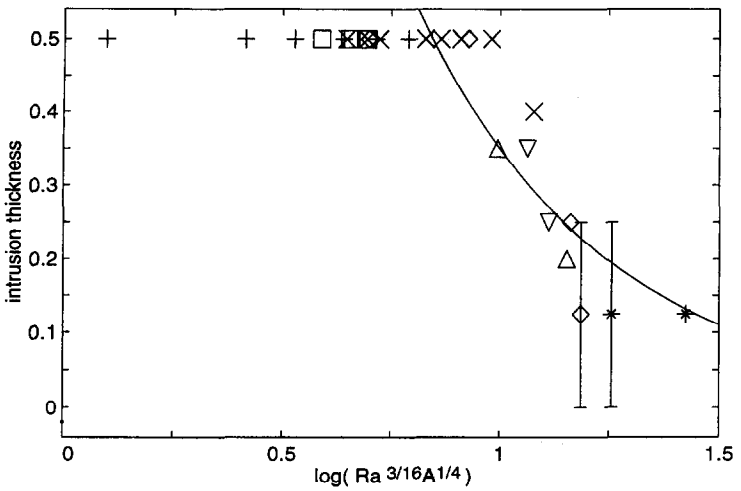

Fig. A1. The height of the stagnant fluid at mid-height vs the criterion $Ra^{-3/16}A^{-1/4}$ as proposed by Patterson and Imberger [11]. Error bars were drawn for the runs with 'strong jets' [14], if we could not recover the velocity profiles. The experimental data were represented by the same symbols as in Fig. 3.

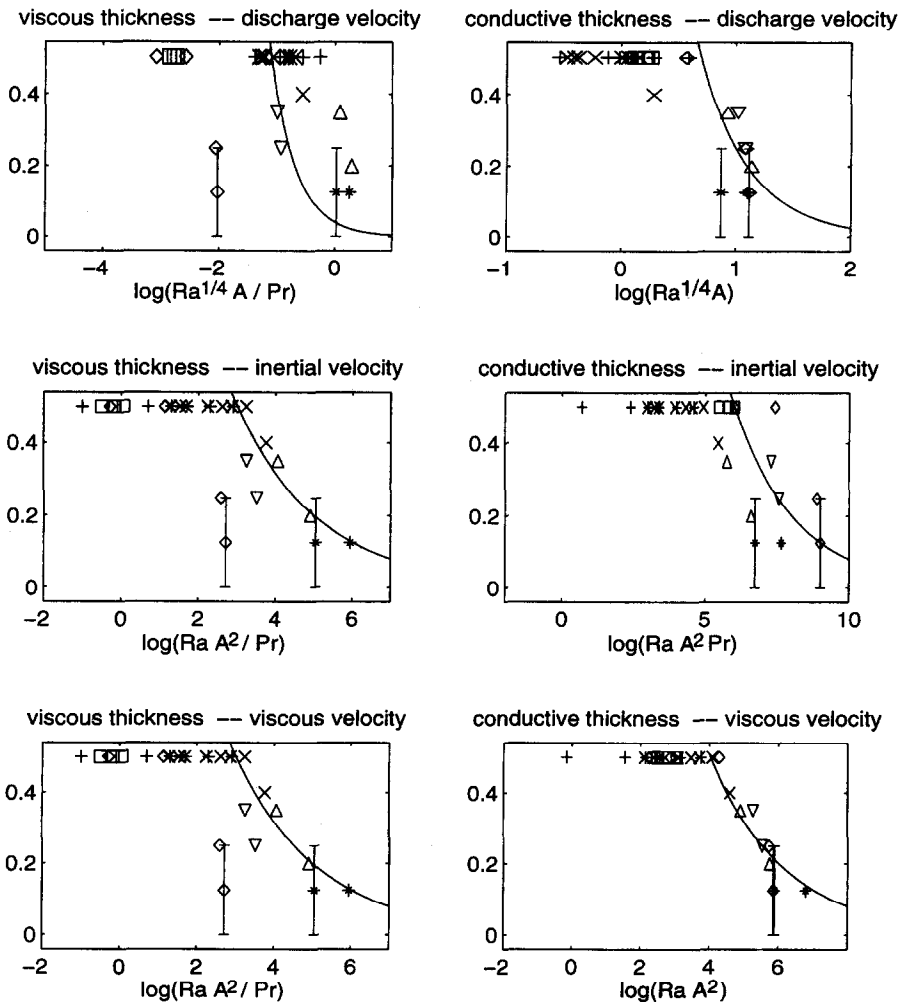

Fig. A2. The various possibilities for a core dominated flowing-layer thickness (see also Table A1). The experimental data were represented by the same symbols as in Fig. 3. Error bars were drawn for the runs with 'strong jets' [14], if we could not recover the velocity profiles.

Table A1. Various possibilities for a core-dominated flowing-layer thickness

Scaling for flowing layer thickness	Viscous spreading	Conductive spreading
$\delta/H =$	$\delta^2 \sim vt \sim vL/U$	$\delta^2 \sim \kappa t \sim \kappa L/U$
Discharge velocity $U \sim \frac{Q}{\delta} \sim \frac{\kappa RA^{1/4}}{\delta}$	$Ra^{-1/4}PrA^{-1}$ (Ivey and Hamblin [17])	$Ra^{-1/4}A^{-1}$ (Bejan *et al.* [14])
Inertial velocity $U \sim (g\alpha T\delta)^{1/2}$	$Ra^{-1/5}Pr^{1/5}A^{-2/5}$	$Ra^{-1/5}Pr^{-1/5}A^{-2/5}$
Viscous velocity $U \sim RA\frac{\kappa}{L}\left(\frac{\delta}{H}\right)^3$	$Ra^{-1/5}Pr^{1/5}A^{-2/5}$	$Ra^{-1/5}A^{-2/5}$ (present approach)

to support this statement we also plot the experimental data against other possible criteria. The depictions will prove that none of those criteria is consistent with the entire set of experimental data (Figs. A1 and A2).

Although only valid for the case $Ra > A^{-12}$, it might be interesting to see how well the Patterson and Imberger [11] scaling works in the range of parameters of the presented experiments. Thus, we included Fig. A1, where the non-dimensional flowing-layer thickness was plotted against $Ra^{-3/16}A^{-1/4}$. The agreement of the scaling with the experimental results is fair, but especially for extremely low values of A ($\times$, [6]), the discrepancy becomes obvious.

A layer thickness for a core dominated flowing-layer thickness is derived as follows. The initial intrusion originating from the hot (cold) plate grows in thickness δ due to either viscous $\sim\sqrt{vt}$ or conductive process $\sim\sqrt{\kappa t}$ (see Table A1). The spreading of the layer thickness with time, i.e. with increasing distance from the hot (cold) plate has been observed in Bejan *et al.* [14]. They also saw evidence for entrainment, which they displayed in their plot of streamlines. The time available for the growth is the advection time through the tank $\tau_a \sim L/U$, using a velocity U which can either be based on the discharge from the hot plate, an inertial velocity scale or last not least a viscous velocity scale.

Some of these approaches are formally identical with previously derived transition criteria for the regime boundary between the transition regime and the convective regime. Figure A2 includes the above scalings (Table A1) as plots, where the solid line represents the scaled thickness (with the factor of proportionality chosen to fit the data as well as possible); the symbols represent the experimental data.

Figure A2 indicates that conduction determines the thickness of the flowing layers. None of the viscous scalings provides a satisfactory result for the flowing layer thickness. The figure also shows that in the case of the included data the velocity scale must be based on viscosity which is in full accordance with the prediction from the scaling.

APPENDIX B

The temperature gradient vs previous criteria

In this paper, we argue that the proposed criterion for the transition from a longitudinally stratified fluid body to a mainly vertically stratified fluid body is governed by the value of RaA^2. We, therefore, propose this criterion for estimating the longitudinal temperature gradient in a long cavity. For comparison, we plotted the data available according to the previously proposed criteria (Fig. B1).

In the graph K_1 against Ra^2A^3 (Fig. B1 upper panel), as proposed by Cormack [4, 5] and Imberger [6], one of the data points by Böhrer [18] ($\bigcirc$) and one of Cormack *et al.*'s ($+$) do not align with the others. In addition, the experimental result are higher than the numerical results, which should not happen, as the experimental results are subject to interference with the isothermal environment, which lowers the measured K_1.

The data points align much better when plotted against $RaA^{12/7}$, as proposed by Daniels [24], but still not as well as in Fig. 4. Finally, we also provide a plot K_1 vs $RaA^{2.5}$ to show that a further increase of the A-exponent beyond 2, does not yield a better collapse of the data than in Fig. 4.

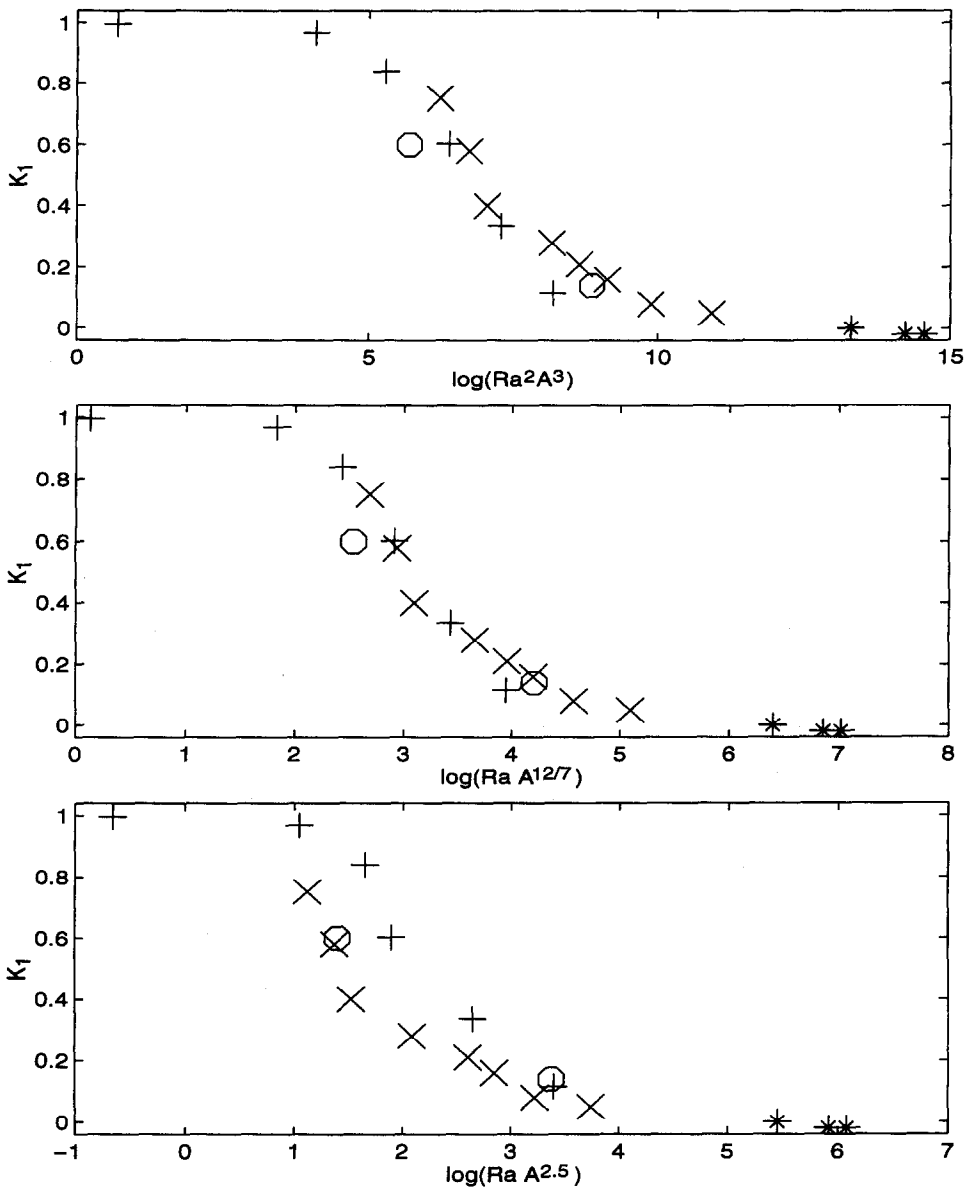

Fig. B1. The experimental data of the longitudinal temperature gradient K_1 against Imberger's [6] criterion (upper panel), Daniels's [24] criterion (middle panel) and against $RaA^{5/2}$ (lower panel). The experimental data points are represented by the same symbols as in Fig. 4.